

The crystal structure of peprossiite-(Ce), an anhydrous REE and Al mica-like borate with square-pyramidal coordination for Al

ATHOS CALLEGARI,^{1,2} FRANCA CAUCIA,^{1,2} FIORENZO MAZZI,² ROBERTA OBERTI,^{1,*} LUISA OTTOLINI,¹ AND LUCIANO UNGARETTI^{1,2}

¹CNR-CS per la Cristallografia e la Cristallografia, via Ferrata 1, I-27100 Pavia

²Dipartimento di Scienze della Terra, Università di Pavia, via Ferrata 1, I-27100 Pavia

ABSTRACT

Single-crystal structure refinements are presented of the holotype of crystal peprossiite-(Ce) (Monte Cavalluccio) and of a new sample from Cura di Vetralla (Viterbo, Italy) with slightly different composition, together with new EMP-SIMS chemical analyses. These results allow us to propose a new unit formula: $[\text{REE}_{1-x-y}(\text{Th}, \text{U})_x \text{Ca}_y](\text{Al}_3\text{O})_{2/3}(\text{B}_{4-z}\text{Si}_z)\text{O}_{10}$ with $x - y + z = 1/3$ ($Z = 1$) for the peprossiite group. Lattice constants for the holotype crystal are: $a = 4.612(1)$, $c = 9.374(3)$ Å, $V = 172.6$ Å³, $Z = 1$, space group $P\bar{6}2m$. The crystal structure was solved by Patterson methods and refined to $R_{\text{obs}} = 1.8\%$ ($R_{\text{all}} = 2.2\%$) for 706 unique reflections in the 2θ -range 6–136°. Lattice constants for the thorian peprossiite-(Ce) from Cura di Vetralla are: $a = 4.596(3)$, $c = 9.309(16)$ Å, $V = 170.3$ Å³, and the structure was refined to $R_{\text{obs}} = 2.9\%$ and $R_{\text{all}} = 3.0\%$ for 271 unique reflections in the 2θ -range 4–80°. The topology of the tetrahedral layer and the site of the inter-layer cation (REE) in peprossiite resembles that of dioctahedral micas. The main difference lies in the presence of layers of pyramids instead of layers of octahedra typical of mica. In peprossiite, Al is coordinated by five O atoms in a nearly square-pyramidal arrangement, the base of which is formed by pairs of apical O atoms from two layers of tetrahedra related by a mirror plane. Three of these pyramids share their apical O forming Al₃O groups with occupancy of 2/3 according to the structure refinement. A model is proposed that explains the apparent disorder in the pyramidal layer of peprossiite by the stacking within a triple cell (with $a' = a\sqrt{3}$ and $\mathbf{a}' = 30^\circ$) of three ordered layers randomly translated by $\pm \mathbf{a}$.

INTRODUCTION

Peprossiite-(Ce), an anhydrous borate of Al and REE, was discovered in 1986 in a “type-A sanidinite” ejectum at Monte Cavalluccio, Campagnano di Roma, Italy. The description of the mineral with its chemical and physical properties was reported by Della Ventura et al. (1993). The determination of the crystal structure of holotype peprossiite-(Ce) (Caucia et al. 1991) was hindered by difficulties in the interpretation of the observed structural disorder at the atomic scale. Substantial differences also were found between the unit formula calculated from the chemical analysis by Della Ventura et al. (1993) and that derived from the crystal structure. A recent discovery of (Th-rich) peprossiite-(Ce) at another locality together with more complete chemical analyses and advances in analytical techniques allow resolution of these problems. We report herein the crystal structure of two peprossiite-(Ce) crystals and model the structural disorder. The re-definition of peprossiite-(Ce) has been approved by the IMA-Commission on New Minerals and Mineral Names (99V). We dedicate this work to the memory of Giuseppe (Pep) Rossi, whom this mineral was named after, in the decennial of his passing away.

EXPERIMENTAL METHODS

Sample description

Holotype peprossiite-(Ce) (crystal Pep1) was described in detail by Della Ventura et al. (1993). The sample recently found (crystal Pep2) occurs inside a foid-bearing syenitic ejectum from Cura di Vetralla, Viterbo, Italy, and is significantly enriched in Th with respect to the holotype. The host rock, collected within a pyroclastic deposit belonging to the Vico volcanic complex, is composed of predominant potassium feldspar with minor plagioclase, augitic clinopyroxene, biotite, and magnetite. Accessory phases include titanite, zircon, and rutile. Thorian peprossiite-(Ce) occurs in the myarolitic cavities resulting from the intersecting potassium feldspar, as fan-shaped aggregates of (flexible) platy, transparent, and lemon-yellow colored crystals with the maximum dimension of 200 μm.

X-ray analysis and data collection

A few crystals from both specimens were selected for crystallographic analysis and X-ray data collection on the basis of optical behavior and freedom from inclusions; they were mounted on a Philips PW-1100 automated four-circle diffractometer and examined with graphite-monochromatized MoK α X-radiation. Crystal quality was assessed via the profiles and widths of Bragg diffraction peaks; only a couple of crystals from each specimen were found to be suitable for data collection. Unit-cell dimensions were calculated from least-

*E-mail: oberti@crystal.unipv.it

squares refinement of the *d*-values obtained from 60 rows of the reciprocal lattice by measuring the center of gravity of reflections in the 2θ range between -70 and 70° (Table 1). Very high (Pep1) and high resolution (Pep2) intensity data of hexagonal-equivalent reflections were collected using the step-scan profile technique of Lehman and Larsen (1974); integration was made by means of profile-fitting analysis. The data were corrected for absorption following the method of North et al. (1968) and for Lorentz and polarization effects, then averaged and reduced to structure factors.

Crystal structure determination and refinement

Most of the experimental details reported in this section concern the holotype crystal of peprossiite-(Ce) from Monte Cavalluccio (Pep1). Due to the presence of heavy atoms in the preliminary analysis (REE, which were found to order at the M2 site), the crystal structure of peprossiite-(Ce) could be solved by Patterson methods in the Laue group *P6/mmm*. On the basis of their reciprocal distances, the four highest maxima were related to vectors between the M2 site and, respectively, the sites occupied by Al, B, and the two independent O atoms, which form tetrahedra centered on B. The unique M2 site was assigned at the origin, and the coordinates of the other maxima are those of M1 (occupied by Al), T (occupied by B), O1, O2 sites in the unit cell. The position of a third O atom (O3 site) was obtained from a subsequent Fourier synthesis.

The number of equipoints for the M1 and O2 sites, as derived from the symmetry of the space group in the Patterson space (*P6/mmm*), is larger than the number of atoms in the unit cell. The space group of peprossiite must be chosen among the acentric space-groups with Laue symmetry *P6/mmm*. Only *P6̄2m* was consistent with an arrangement of O1 (unshared) and O2 (shared) O atoms in a sheet of borate tetrahedra. The ideal formula unit derived from site multiplicity in space group *P6̄2m* is (REE)Al₃(B₄O₁₀)O; this formula shows an excess of positive charges (+2), possibly related to an excess of Al.

The structure refinement utilized a full-matrix least-squares program; scattering factors for neutral atoms were used at the M2 (REE), M1 (Al), and T (B) cation sites, whereas those for partially ionized O atoms (O⁻) were used at the anion sites. A

first unweighted refinement performed on 640 observed reflections [*I* ≥ 2σ_{*I*}] with fixed occupancies as derived from preliminary chemical analysis converged to *R*_{obs} = 6.2%; a mixture of 0.914 Pr + 0.086 Ca was used at M2, as Pr has a similar number of electrons to the aggregate trivalent and tetravalent cations at M2 obtained from the chemical analysis reported by Della Ventura et al. (1993). Abnormally high displacement factors were observed at the M1 and O3 sites, suggesting their incomplete occupancy. Accordingly, occupancies of all the sites but M2 and T were allowed to vary. The *R*_{obs} factor dropped to 3.5%; the M1 and O3 occupancies approached 2/3 (actually, 0.65(1) and 0.67(3), respectively), whereas those of O1 and O2 remained equal to 1.0. At this point, the ideal formula unit was (REE)Al₂(B₄O₁₀)O_{2/3}, and the charge unbalance was -0.33.

The positions and multiplicities of the M2, T, O1, and O3 sites in space group *P6̄2m* are also consistent with those in the centric space-group *P6/mmm*; in the latter, however, the multiplicities of M1 (3) and of O2 (6) are doubled. The centric symmetry of most of the atoms suggested that Al and O could be distributed over equivalent centric M1 and O2 sites. This possibility was investigated by using an option of the least-squares program, which allows refinement of the possible partition of some atoms between centric sites in an acentric crystal. The refinement ended (*R*_{obs} = 2.0%) with Al equally distributed [0.52(3) vs. 0.48] over the six centric M1 sites (1/3 occupancy) in *P6/mmm* and not over the three M1 sites (2/3 occupancy) in *P6̄2m*. A limited distribution of the O over centrosymmetric sites was observed also for the O2 site [0.92(2) vs. 0.08]. In conclusion, only the symmetry of the O2 site is really acentric in the crystal structure of peprossiite.

The occupancy of Pr was subsequently allowed to vary against that of Ca at the M2 site, together with the occupancy of B against that of Si at the tetrahedral T site. The changes in the refined site-scattering were very small, and *R*_{obs} converged to 1.8%, whereas *R*_{all} for the 706 independent reflections converged to 2.2%.

The site scatterings at the cation sites are accurate within 5%; the refined values at M2 (55.0 epfu) and at T (5.3 epfu) suggest incorporation of small amounts of lighter (Ca and Y) and heavier (Si) elements, respectively.

The structure refinement of a crystal from the second specimen (Pep2) was done following the above procedure, except for the choice of scattering factors at the M2 site. Initially, the M2 occupancy was kept fixed to (La 0.9 + Th 0.1) based on a preliminary chemical analysis. The results were comparable to those of the refinement of crystal Pep1, although the quality of the second crystal was lower. The occupancies at the M1 and O3 sites converged to 2/3, and Al was equally distributed over 1/3 of the six centrosymmetric sites; however, no disorder over enantiomorphic sites was found for O2 in crystal Pep2, as the O atoms occupy uniquely and completely the sites compatible with the acentric space group *P6̄2m*. No Si was indicated at the tetrahedral site, whereas the Th content at the M2 site was higher [Th 0.22(4) vs. La 0.78], giving 5.0 epfu at T and 64.1 epfu at M2. *R*_{all} converged to 3.0%.

Atomic coordinates and equivalent isotropic displacement parameters for the two refined crystals are listed in Table 2; selected bond lengths and angles are listed in Table 3. The larg-

TABLE 1. Unit-cell parameters, data-collection parameters, and selected refinement parameters for the crystals of peprossiite-(Ce) from the holotype specimen (Pep1) and from the new finding from Cura di Vetralla (Pep2)

	Pep1	Pep2
Crystal size (μm ³)	260 × 100 × 24	160 × 130 × 80
<i>a</i> (Å)	4.612(1)	4.596(3)
<i>c</i> (Å)	9.374(3)	9.309(16)
<i>V</i> (Å ³)	172.7	170.3
<i>Z</i>	1	1
Space group	<i>P6̄2m</i>	<i>P6̄2m</i>
2θ range (°)	4–134	4–80
<i>hkl</i> range	± <i>h</i> , ± <i>k</i> , <i>l</i>	± <i>h</i> , ± <i>k</i> , ± <i>l</i>
scan mode	ω	ω - 2θ
scan width (°)	2.0	2.0
scan speed (°)	0.05	0.03
No. collected <i>F</i>	6265	4263
No. unique <i>F</i>	706	271
<i>R</i> _{sym} (%)	4.5	5.8
No. obs <i>F</i> (<i>I</i> > 2σ _{<i>I</i>})	640	269
<i>R</i> _{obs} (%)	1.8	2.9
<i>R</i> _{all} (%)	2.2	3.0

est differences between the two set of data are in the atomic coordinates of O2 (Δx 0.0035, Δz 0.0020) and in the <M2-O> mean bond-length (2.764 Å in Pep1, 2.742 Å in Pep2); this latter feature is consistent with a higher content of a smaller tetravalent cation (Th) at the M2 site. The <T-O> and <M1-O> mean bond lengths are identical within the experimental errors. The anisotropic displacement parameters and observed and calculated structure factors are listed in Tables 4 and 5¹.

Chemical analyses of the refined crystals

The holotype crystal used for the structure refinement was embedded in epoxy-resin, polished and analyzed with both the electron- and the ion-microprobes (EMP and SIMS).

WDS-EMP analyses were done with a Jeol JXA 840A probe at the Centro Grandi Strumenti of the Università di Pavia. Si, Al, and Ca were quantified by using minerals as standards:

¹For a copy of Table 5, document item AM-00-038, contact the Business Office of the Mineralogical Society of America (see inside front cover of recent issue) for price information. Deposit items may also be available on the American Mineralogist web site (<http://www.minsocam.org> or current web address).

TABLE 2. Atomic coordinates and equivalent isotropic B_{eq} (Å²) in peprossiite-(Ce)

Site	Mult.	Occup.	<i>x/a</i>	<i>y/b</i>	<i>z/c</i>	B_{eq}
M2	1	*	0	0	0	0.86(0)
			0	0	0	0.67(1)
M1	3	2/3	0.3889(2)	0	1/2	0.40(2)
			0.3889(9)	0	1/2	0.52(7)
T	4	†	1/3	2/3	0.2202(1)	0.57(1)
			1/3	2/3	0.2196(1)	0.49(7)
O1	4	1	1/3	2/3	0.3754(1)	0.63(1)
			1/3	2/3	0.3744(4)	0.68(5)
O2	6	1	0.4215(3)	0	0.1612(1)	0.81(2)
			0.4180(9)	0	0.1592(4)	0.81(7)
O3	1	2/3	0	0	1/2	0.47(3)
			0	0	1/2	0.53(17)

Note: B_{eq} is calculated from refined anisotropic parameters. First line = Pep1; second line = Pep2.

* Pep1: Pr 0.898(2), Ca 0.102; Pep2: La 0.785(11), Th 0.215.

† Pep1: B 0.967(3), Si 0.033; Pep2: B 1.000.

TABLE 3. Selected interatomic distances (Å) and angles (°) in peprossiite-(Ce)

		Pep1	Pep2
M2 ditrigonal prism			
M2-O2	×6	2.462(1)	2.426(4)
M2-O2	×6	3.066(1)	3.058(4)
<M2-O2>		2.764	2.742
O2-O2-O2		89.59(5)	88.3(1)
O2-O2-O2		150.41(7)	151.7(1)
T (B) tetrahedron			
T-O1		1.455(1)	1.442(7)
T-O2	×3	1.486(1)	1.489(5)
<T-O>		1.478	1.478
O1-T-O2	×3	111.86(5)	112.2(2)
O2-T-O2	×3	106.99(5)	106.6(2)
M1 (Al) pyramid			
M1-O1	×4	1.844(1)	1.840(3)
M1-O3		1.793(1)	1.788(3)
<M1-O>		1.834	1.830
O1-M1-O1	×2	78.62(2)	78.85(8)
O1-M1-O1	×2	92.45(3)	92.26(10)
O1-M1-O3	×4	106.14(3)	106.11(10)

TABLE 4. Anisotropic displacement coefficients ($\times 10^4$) in peprossiite-(Ce)

Site	U_{11}	U_{22}	U_{33}	U_{13}
M2	122(1)	122(1)	83(1)	0
	84(2)	84(2)	86(2)	0
M1	46(2)	48(3)	60(2)	0
	56(11)	44(13)	96(11)	0
T	78(3)	78(3)	59(3)	0
	52(10)	52(10)	82(16)	0
O1	92(2)	92(2)	54(2)	0
	90(9)	90(9)	78(12)	0
O2	131(3)	72(3)	87(2)	-30(2)
	101(11)	34(13)	149(13)	-20(12)
O3	46(4)	46(4)	86(7)	0
	30(23)	30(23)	141(46)	0

Notes: U_{12} is fixed to $1/2 U_{22}$ and U_{23} to 0 by symmetry. First line: Pep1; second line: Pep2. The atomic displacement parameter is of the form: $\exp[-2\pi^2(h^2a^2U_{11} + k^2b^2U_{22} + l^2c^2U_{33} + 2hka'b'U_{12} + 2hla'c'U_{13} + 2klb'c'U_{23})]$.

pyrope Dora Maira (SiK α , AlK α), diopside Wakefield (CaK α). Analytical conditions were 20 kV and 20 nA beam current, and 5 μ m beam diameter. Tabulated data are averages of ten analyses, which are representative of crystal composition and zoning. Data reduction was done using the PAP $\phi(\rho Z)$ routine (Pouchou and Pichoir 1985).

Ion-probe analyses were done with a Cameca IMS 4f probe on polished crystals coated with gold (~ 400 Å thickness) bombarded with a ¹⁶O primary beam. Experimental conditions and calibration procedures for REE, Th, and B are briefly described below. Further details can be found in the cited references.

REE, Y, and Th. REE (La, Ce, Pr, Nd, Sm, Eu, Gd, Dy, Er, Yb), Y, and Th signals were measured with a 3 nA current focused onto a spot of ~ 4 – 5 μ m in diameter. The width of the energy slit was 50 eV and the voltage offset applied to the sample accelerating voltage (+ 4500 V) was -100 V. The REE-enriched Ca-Al-Si-glasses prepared by Drake and Weill (1972) and the NIST610 glass standard were used to convert relative ion intensities to elemental concentrations in the case of REE and Y, whereas NIST610 and other synthetic glasses (kindly provided by K. Schmidt, Göttingen) were used for Th. Al was assumed as the internal reference element. Interferences in the M- and H-REE region of the secondary ion spectrum were significant (especially in crystal Pep1); complex molecular interferences were carefully removed according to the procedure reported in Oberti et al. (1999). The accuracy of the SIMS analyses is estimated to be $\sim 10\%$ relative for REE and Y, and 10–15% relative for Th.

Light elements. B was analyzed by the procedure developed for silicates by Ottolini et al. (1993), which involves an empirical approach and energy-filtering. Synthetic glass standards were used (Pyrex, NaAlB, and NIST610, which are representative of our calibration curve). The accuracy of the SIMS analyses for B was shown to be better than $\pm 3\%$ (Hawthorne et al. 1995); in the present case, it seems to be even higher ($\sim 1\%$) when compared to the stoichiometric value (4.00 in Pep2).

Complete chemical analyses were obtained for crystal Pep1 by combining EMP and SIMS results. As SIMS analyses consumed all the available material in the case of Pep2, we used the Al and Ca contents measured on crystal Pep1. Oxide percentages and unit formulae calculated on the basis of seven cations per formula unit (pfu)—as suggested from the struc-

ture refinement—are reported in Table 6, together with the refined site-scatterings and those calculated from the unit formulae. A comparison with the analysis reported by Della Ventura et al. (1993), after their recalculation to 9 oxygen atoms pfu (column 1 in Table 6), shows that those authors had probably underestimated the B content. Inspection of the formula unit derived from the structure refinement of peprossiite reveals an analogy with dioctahedral mica; an important difference is the absence of the two OH groups of micas, which are replaced by 0.67 O in peprossiite. Different chemical species occur in the two minerals: in peprossiite B replaces Si, Al, and Ti in the T tetrahedra, and REE replace monovalent and divalent M2 inter-layer cations in mica.

CRYSTAL STRUCTURE, CATION ORDERING, AND LAYER STACKING IN PEPROSSIITE

Peprossiite is a layered borate, with layers of six-membered rings of B tetrahedra alternating with inter-layer cations (REE) and layers of Al polyhedra; the stacking sequence closely resembles that in micas (Fig. 1). Thus peprossiite has an entirely new type of structure for a borate, according to the structural classification of Hawthorne et al. (1996). The layer of tetrahedra (Fig. 2a) is topologically identical to that of mica (Bailey 1984). Consequently, the length of the *a* cell-edge in peprossiite-(Ce) (4.61 Å) is similar to that of the corresponding edge of muscovite (5.18 Å) multiplied by the ratio (0.90) between the <B-O> and <(Si,Al)-O> mean bond lengths (4.66 Å).

However, the stacking of the layers of tetrahedra along the [001]-direction is different from that of mica: adjacent layers are reciprocally rotated in micas, but are related by mirror planes parallel to (001) in peprossiite. Due to the peculiar stacking of the layers of tetrahedra, the coordination around the inter-layer M2 site is still twelve but has the shape of a ditrigonal prism (Fig. 1). This coordination is different from that observed around monovalent and divalent cations in the most common micas (2M₁ polytype), where twelve O atoms (actually, two sets of six O atoms) are the vertices of two intersecting octahedra with

different sizes. The arrangement found in peprossiite is similar to that observed in the rare 2M₂ polytype (e.g., in nanpingite, the cesian analogue of muscovite; Ni and Hughes 1996).

From a crystal-chemical perspective, the main difference between peprossiite and mica is the lower coordination of the M1 cation, which is surrounded by five O atoms arranged at the vertices of a nearly tetragonal pyramid in peprossiite.

The M1 coordination is related with the stacking of the layers of tetrahedra. Two pairs of superimposed apical O1 atoms from adjacent layers of tetrahedra form the nearly square base

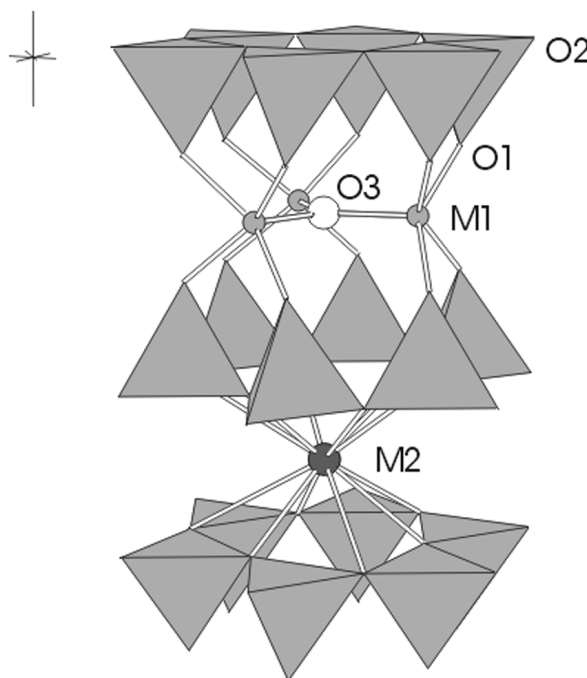


FIGURE 1. Clinographic view of the crystal structure of peprossiite showing the coordination of M1 and M2 cations.

TABLE 6. Chemical analyses of peprossiite-(Ce)

Atom	wt% oxides			Unit formulae		
	1	2	3	1	2	3
Ce	18.62(62)	18.79(61)	15.27(18)	0.40	0.46	0.37
La	14.53(66)	13.75(65)	8.58(39)	0.32	0.34	0.21
Pr	4.37(18)	1.20(05)	1.21(05)	0.09	0.03	0.03
Nd	2.11(nd)	2.07(06)	2.82(13)	0.05	0.05	0.07
Th	1.68(47)	2.35(17)	14.29(61)	0.02	0.04	0.22
Ca	1.34(09)	1.20(35)	[1.20]	0.09	0.09	0.09
Σ(Sm-Yb,Y)		0.17	0.55		<0.01	0.02
ΣM2				0.97	1.01	1.01
Al (M1)	29.40(22)	26.16(79)	[26.16]	2.04	2.05	2.04
B	29.56(17)	32.80(99)	34.70(90)	3.00	3.77	3.96
Si	—	2.75(18)	—	—	0.18	—
Totals	101.61	101.24	104.78			
O				9.00	10.57	10.57
M2	ssr	55.0	64.1	ssc	56.2	61.0
M1	ssr	26.0	26.0	ssc	26.7	26.5
T	ssr	21.2	20.0	ssc	21.4	19.8

Notes: Columns 1 and 2, from the holotype specimen, obtained by combining electron- and ion-probe results. Column 3 reports ion-probe analyses of the sample from Cura di Vetralla. The refined site-scatterings (ssr, epfu) at the cation sites are compared to those calculated from the unit formulae (ssc). (1) Analysis after Della Ventura et al. (1993); unit formulae calculated on the basis of 9 O pfu. (2, 3) This work; oxides weight percent recalculated on the basis of seven cations pfu. The accuracy of the ion-probe results is better than 10% rel. for B and REE and 10–15% rel for Th.

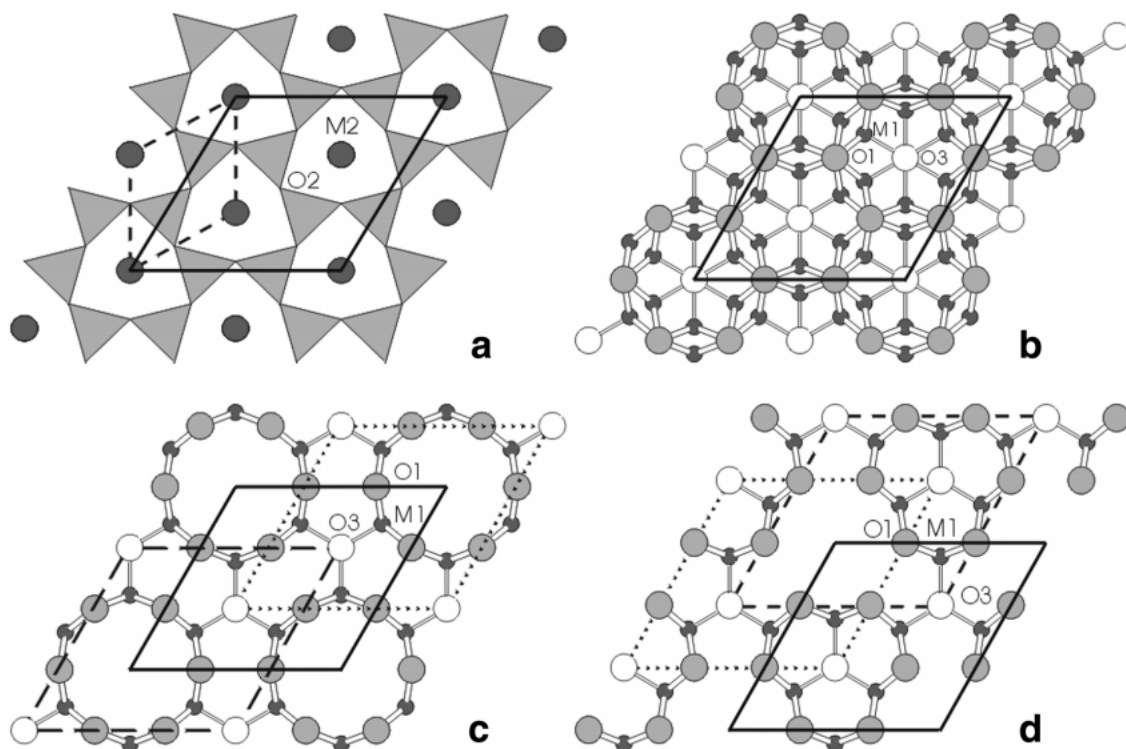


FIGURE 2. Projections along [001] of the crystal structure of peprossiite. (a) The layer of tetrahedra and the inter-layer M2 cations. Dashed lines: projection of the real unit-cell; full lines: projection of the triple cell with $a' = a\sqrt{3}$ and $\mathbf{a}' \wedge \mathbf{a}' = \sim 30^\circ$. (b) The layer of pyramids. The centric disordered arrangement of atoms at M1 (dark gray), O1 (gray) and O3 (white) sites when Al (1/3 occupancy at M1) and O (2/3 occupancy at O3) randomly distribute over all the available positions in space group $P6/mmm$. The O1 sites (i.e., the apical O atoms of the tetrahedra) are fully occupied. (c) The layer of pyramids. The centric ordered arrangement of fully occupied M1, O1, and O3 sites. In this projection of the triple cell (full lines), Al_2O groups fill the hexagonal prismatic cavities around the triad axes at $1/3\ 2/3$ and $2/3\ 1/3$. The third cavity around the triad axis at $0\ 0$ is empty. Within this model, the shortest Al-Al distances are 2.82 and 3.11 Å. Dotted and dashed lines indicate alternative triple-cells translated by $\pm \mathbf{a}$. The origin of the triple cells always coincides with the origin of the true unit-cell. (d) The layer of pyramids. The acentric ordered arrangement of the same sites in the triple cell (space group $P6m2$). Within this model, the shortest Al-Al distances are 2.47 and 3.11 Å. Alternative triple cells are as in c.

of the pyramid surrounding M1 in peprossiite. The base is parallel to [001], and its edges are 2.34 and 2.66 Å (respectively, parallel and perpendicular to [001]). The O3 site at the vertex of the pyramid is on the 6 axis, and is shared by three pyramids (Fig. 1). The layer of octahedra of micas thus becomes a layer of pyramids in peprossiite.

Few minerals contain Al in fivefold coordination; the best known is andalusite, in which the O atoms are arranged at the vertices of a nearly trigonal dipyramid. The presence of Al in fivefold coordination has been reported by Udawaga et al (1974) in a muscovite dehydroxylated after annealing in air; it was recently confirmed in paragonite dehydroxylated in the same way at 600 °C (P. Comodi, personal communication; Comodi and Zanazzi 2000). The dehydroxylation process can be locally described as the substitution of two OH groups related by the center of symmetry by one O atom at the center of symmetry (Or). In fully dehydroxylated dioctahedral micas, however, the layer maintains the pattern and the dimensions of the six-membered rings of Al-centered polyhedra, in which 1/3 of the connections is by corner-sharing, and not by edge-sharing. This conservation of the fundamental structure arrangement allows

re-hydroxylation of muscovite when the dehydroxylation process is not complete [cf. Guggenheim et al. (1987) and Mazzucato et al. (1999) for structural and kinetic models of this process]. Therefore the geometry of the coordination of $^{[5]}\text{Al}$ in dioctahedral dehydroxylated micas is necessarily different from that observed in peprossiite, i.e., a distorted trigonal dipyramid; at nearly equal $\langle \text{Al-O} \rangle$ distances (1.835 vs. 1.834 Å), the Al-Or distance in dehydroxylated paragonite is 1.672 Å (P. Comodi, personal communication) to be compared with Al-O3 equal to 1.793 Å in peprossiite-(Ce). Moreover, the ordering of the Al_2O clusters peculiar of peprossiite (discussed below) implies a more complex pattern of rings of Al-centered polyhedra. The Or atom in dehydroxylated micas is shared by two Al atoms, whereas the O3 atom in peprossiite is shared by three Al atoms. As a consequence, in peprossiite six-membered rings of polyhedra linked through O1 are surrounded by four-membered rings of polyhedra linked through O3 (Fig. 2c).

Another difference between the crystal structure of peprossiite and that of dioctahedral micas involves the distribution of the vacant sites in the layer of pyramids. In dioctahedral micas, the Al-filled sites are crystallographically

distinct from the vacant site; in peprossiite, the vacant site is apparently distributed randomly over one out of three (or over two out of six in $P6/mmm$) equivalent M1 sites (Fig. 2b). However, the partial occupancy of the O3 site (the vertex of the M1 pyramid), which is equal to that of the M1 site, also suggests that in peprossiite the vacant sites are ordered.

A model for Al ordering within the layer is obtained by describing the peprossiite structure with a triple hexagonal cell with $a' = a\sqrt{3}$ and $\mathbf{a} \wedge \mathbf{a}' = 30^\circ$ (Fig. 2c). If we take into account the centric symmetry ($P6/mmm$) of this layer as shown by the structure refinement, the six partly vacant M1 sites (with coordinates $0.39\ 0\ 1/2$) become three sets of six sites (with coordinates $2x\ x\ 1/2$) in the triple cell. The partial ($1/3$) occupancy of the M1 sites in the smaller unit-cell can be explained in terms of the triple cell by complete ordering of the Al atoms in one out of these three sets of sites. Actually, two of them have M1-M1 distances (1.02 Å and 1.8 Å, respectively) that are too short to allow for simultaneous occupancy locally. On the contrary, the shortest M1-M1 distances in the third set (with coordinates $0.40\ 0.20\ 1/2$) are 2.82 Å (between cations in pyramids sharing the O1-O1 edge) and 3.11 Å (between cations in pyramids sharing the O3 vertex), which are comparable with the analogous distances observed in micas (2.95–3.00 Å) for cations occurring in edge-sharing octahedra. The unique O3 site in the smaller cell (with coordinates $0\ 0\ 1/2$), splits into two sets of sites in the triple cell, which have multiplicity 1 and 2, respectively (and coordinates $0\ 0\ 1/2$ for the first and $1/3\ 2/3\ 1/2$ plus $2/3\ 1/3\ 1/2$ for the second set). The two O3 sites of the second set are exactly the vertices of the pyramids formed around the six sites which are suitable for Al incorporation; the observed $2/3$ occupancy in the smaller unit-cell can therefore be explained by these two O3 sites being fully occupied (Fig. 2c).

Within this model, the layer of pyramids in peprossiite would be formally obtained by inserting an Al_2O group into two of the three hexagonal prismatic cavities, which are formed around the triad axes of the triple cell by the O1 apical O atoms from two adjacent layers of tetrahedra (Fig. 2c). The third prismatic cavity must be vacant to avoid both too short Al-Al distances in adjacent hexagonal cavities and severe overbonding on the O1 sites. The $2/3$ occupancy for M1 and O3 sites of the $P\bar{6}\ 2m$ unit-cell is thus the maximum occupancy allowed by the structure.

Thus the difference between the crystal chemistry of micas and that of peprossiite originates from the constraint of equal M1 and O3 occupancies. In micas, the vacancy occurs only in the sites available for the Al cations, and it does not concern the O atoms not linked to tetrahedra (i.e., the hydroxyl groups). In peprossiite, all the sites (O included) of a potential Al_2O group must be simultaneously vacant.

To test the reliability of the proposed model, an accurate search for further X-ray reflections due to the presence of the triple cell was performed with a rotating-anode generator working at 5 kW, but none were found. This experimental evidence could be obviously explained by a random arrangement of the vacancies in M1 and O3 sites within each layer of pyramids. According to the observed $2/3$ occupancy for both M1 and O3, this disorder would require random insertion of Al_2O groups into $2/3$ of the O1 hexagonal prismatic cavities of the layer; this is almost impossible without locally producing either short

Al-Al distances or overbonding on the O1 sites. To avoid it, many of the Al_2O groups should be substituted by Al_2O or perhaps AlO groups; however, this situation would produce a decrease of the Al occupancy with respect to that observed for the O3 sites, and also a diffuse local charge unbalance. The hypothesis of a disorder within the layer of pyramids should be therefore discarded.

The absence of reflections attributable to a triple cell can also be explained by the stacking of equal layers, each ordered in terms of the above model, but with the center (O3) of the Al_2O vacant sites randomly shifted on one of the three available positions ($0\ 0\ 1/2$, $1/3\ 2/3\ 1/2$, and $2/3\ 1/3\ 1/2$) of the triple cell that derive from the unique O3 site in the smaller unit-cell (Fig. 2c, cells defined by full, dashed, and dotted lines respectively). These three equally ordered arrangements of atoms are related by translations along vectors $+\mathbf{a}$ and $-\mathbf{a}$ respectively, where \mathbf{a} is parallel to the edge of the single unit-cell. The stacking of ordered layer of pyramids randomly translated according to $+\mathbf{a}$ or $-\mathbf{a}$ may remove any trace of the triple cell in the observed diffraction pattern.

The above model for the disorder in the peprossiite structure could hold also if the symmetry of the ordered layers were acentric. Figure 2d shows the acentric arrangement of six Al atoms in the triple cell compatible with the results of the structure refinement. As for the centric layer, three identical acentric arrangements of atoms can be obtained by $\pm \mathbf{a}$ translations of the origin of the triple cell (Fig. 2d, cells defined by full, dashed, and dotted lines, respectively). The random stacking of these three acentric arrangements would again produce the observed $2/3$ occupancies for the M1 and O3 sites in the disordered structure. However, the observed centric symmetry of the layer could be obtained only if the atoms were arranged in sites centro-symmetrical to those given in Figure 2d in half (or in nearly half) the stacked layers. If the number of these "enantiomorphic layers" were not equal, a differing partition of the Al atoms between centro-symmetrical M1 sites would have been observed during the structure refinements. On the contrary, both crystals show identical Al occupancies for the pairs of centro-symmetrical M1 sites. Thus, the presence of a centric symmetry between the atoms of each layer is a more convincing explanation of the structural results than the stacking of an equal number of acentric layers in two centro-symmetric arrangements. Furthermore the presence of a shorter M1-M1 distance (2.47 Å instead of 2.82 Å) for cations in pyramids sharing the O1-O1 edge makes the acentric arrangement of Figure 2d even less likely.

Table 7 shows a bond-valence analysis for peprossiite calculated with $2/3$ occupancy of the M1 and O3 sites.

The limited distribution of O2 atoms between centro-symmetric sites, which has been observed during the refinement of the crystal structure of Pep1 (0.92(2) vs. 0.08), implies that some disorder can also affect the stacking of the layers of tetrahedra. The refined occupancies suggest that in 8% of these layers, randomly distributed in the crystal structure, the O of the tetrahedral sheet occupy positions that are the centro-symmetrical equivalents of the corresponding sites in the majority of the layers. Only the O2 atoms show this disorder, because the O1 atoms (and the T cations) fall on the triad axes and are

thus invariant for the two enantiomorphic orientations of the layer. Therefore, these two orientations are simply related by a $\sim\pm 30^\circ$ rotation around the triad axis of all the tetrahedra.

Whereas the disorder involving the layers of pyramids is apparently an intrinsic feature of the crystal structure of peprossiite, the disorder in the stacking of the layers of tetrahedra seems to be a peculiarity of only some specimens (e.g., Pep1); no evidence of this disorder has in fact been detected in crystal Pep2. The presence of 1/3, 2/3 occupancies in trigonal or hexagonal space-groups might suggest the presence of twinning. The only twin law compatible with experimental evidence is 1/3 2/3 0 and 2/3 1/3 0 translation in the triple cell. However, only twin domains of few unit cells along *c* would be consistent with the absence of triple-cell reflections in peprossiite. Therefore, only the complex intra-layer order discussed above is a rational explanation of all the experimental evidence.

Peprssiite may be considered as an end-member in a series of dioctahedral layer structures defined by pyrophyllite, muscovite, margarite, and peprossiite. In this series, the formal charge of the tetrahedral cation decreases: $4 \rightarrow 3.75 \rightarrow 3.5 \rightarrow 3$, with the unshared O atoms becoming more underbonded, and the shared O atoms more overbonded (Table 8). This unbalance could destabilize the structure if the octahedral coordination of M1 were maintained in peprossiite. In peprossiite, the presence of trivalent M2 inter-layer cations improves the balance on the shared O atoms, and the lowering in M1 coordination allows a suitable charge balance on the unshared O atoms.

According to the results of the crystal structure, the ideal unit formula of peprossiite is $\text{REE}(\text{Al}_x\text{O})_2(\text{B}_2\text{O}_5)_2$, where *x* is the occupancy of the M1 and O3 sites. As all the cations at the M2, M1, and T sites are trivalent, the neutrality of the formula would require $x = 5/7 = 0.714$, instead of the maximum value allowed by the crystal structure ($2/3 = 0.667$). A reduction of *x*

TABLE 7. Bond-valence analysis of peprossiite

	M2	M1 (*)	T	Total
O1		$0.395 \times 3 \rightarrow$ $\times 4 \downarrow$	0.83	2.01
O2	$0.40 + 0.08$ $\times 6 \downarrow$		$0.75 \times 2 \rightarrow$ $\times 3 \downarrow$	1.98
O3 (*)		$0.45 \times 3 \rightarrow$		1.35
Total	2.88	2.03	3.08	

Notes: calculated after Brown and Altermatt (1985) and Brese and O'Keeffe (1991).

* Site occupancy: 2/3.

TABLE 8. Idealized bond-valence arrangement for regular polyhedra in T-tetrahedral, M1-dioctahedral layer structures

	Pyrophyllite	Muscovite	Margarite	Peprssiite
Bond strengths				
From T	+4/4	+3.75/4	+3.5/4	+3/4
From M1	+3/6	+3/6	+3/6	+3/5
From M2	0	+1/6	+2/6	+3/6
Unshared O atoms				
From T	1.0	0.938	0.875	0.75
From M1 $\times 2$	1.0	1.000	1.000	1.20
Total	2.0	1.938	1.875	1.95
Shared O atoms				
From T $\times 2$	2.0	1.875	1.750	1.50
From M2	0.0	0.166	0.333	0.50
Total	2.0	2.041	2.083	2.00

can only be attained when tetravalent cations substitute for trivalent [e.g., Si for B and/or (U, Th) for REE]. The former crystal-chemical mechanism is active in crystal Pep1 from the holotype specimen, whereas the latter mechanism is active in crystal Pep2. With *x* fixed at 2/3 and no divalent cations in the formula, charge balance is attained by incorporation of one tetravalent atom per each triple cell, i.e., either 1/12 Si per each T site or 1/3 (Th, U) per each M2 site. The incorporation of some Ca at the M2 site is also possible, and is balanced by that of further amounts of tetravalent cations.

The results reported in this paper thus permit us to propose the new unit formula for peprossiite: $[\text{REE}_{1-x-y}(\text{Th,U})_x \text{Ca}_y](\text{Al}_3\text{O})_{2/3}(\text{B}_{4-z}\text{Si}_z\text{O}_{10}]$ with $x - y + z = 1/3$ ($Z = 1$).

ACKNOWLEDGMENTS

G. Della Ventura (Rome) is gratefully acknowledged for having provided some years ago the holotype specimen of peprossiite-(Ce) from Campagnano di Roma and, recently, the new specimen from Cura di Vetralla, very soon after it was found by Salvatore Fiori, a distinguished amateur mineralogist. Peter C. Burns and Edward S. Grew are also gratefully acknowledged for constructive criticisms during the review process.

REFERENCES CITED

- Bailey, S.W. (1984) Crystal chemistry of the true micas. In *Mineralogical Society of America Reviews in Mineralogy*, 13, 1–57.
- Brese, N.E. and O'Keeffe, M. (1991) Bond-valence parameters for solids. *Acta Crystallographica*, B47, 192–197.
- Brown, I.D. and Altermatt, D. (1985) Bond-valence parameters obtained from a systematic analysis of the inorganic crystal structure database. *Acta Crystallographica*, B41, 244–247.
- Caucia, F., Callegari, A., and Ungaretti L. (1991) La struttura cristallina della peprossiite. *Plinius*, 6, 127–128 (abstract).
- Comodi, P. and Zanazzi, P.F. (2000) Structural thermal behaviour of paragonite and its dehydroxylate: a high-temperature crystal study. *Physics and Chemistry of Minerals*, in press.
- Della Ventura G., Parodi G.C., Mottana, A., and Chaussidon, M. (1993) Peprssiite-(Ce), a new mineral from Campagnano (Italy): the first anhydrous rare-earth-element borate. *European Journal of Mineralogy*, 5, 53–58.
- Drake, M.J. and Weill, D.F. (1972) New rare earth element standards for electron microprobe analysis. *Chemical Geology*, 10, 179–181.
- Guggenheim, S., Chang, Y-H., and Foster van Groos, A.F. (1987) Muscovite dehydroxylation: high temperature studies. *American Mineralogist*, 72, 537–550.
- Hawthorne, F.C., Cooper, M., Bottazzi, P., Ottolini, L., Ercit, S.T., and Grew, E.S. (1995) Micro-analysis of minerals for boron by SREF, SIMS and EMPA: a comparative study. *Canadian Mineralogist*, 33, 389–397.
- Hawthorne, F.C., Burns, P.C., and Grice, J.D. (1996) The crystal chemistry of boron. In *Mineralogical Society of America Reviews in Mineralogy*, 33, 41–116.
- Lehman, M.S. and Larsen, F.K. (1974) A method for location of the peaks in stepscan measured Bragg reflection. *Acta Crystallographica*, A30, 580–586.
- Mazzuccato E., Artioli G., and Gualtieri A. (1999) High temperature dehydroxylation of muscovite-2M₁: a kinetic study by in situ XRPD. *Physics and Chemistry of Minerals*, 26, 375–381.
- Ni, Y. and Hughes, J.M. (1996) The crystal structure of nanpingite-2M₂, the Cs end-member of muscovite. *American Mineralogist*, 81, 105–110.
- North, A.C.T., Phillips, D.C., and Mathews, F.S. (1968) A semi-empirical method of absorption correction. *Acta Crystallographica*, A24, 351–359.
- Oberti, R., Ottolini L., Camara F., and Della Ventura G. (1999) Crystal structure of non-metamict Th-rich hellandite-(Ce) from Latium (Italy) and crystal chemistry of the hellandite-group minerals. *American Mineralogist*, 84, 913–921.
- Ottolini, L., Bottazzi, P., and Vannucci, R. (1993) Quantification of lithium, beryllium and boron in silicates by Secondary Ion Mass Spectrometry using conventional energy filtering. *Analytical Chemistry*, 65, 1960–1968.
- Pouchou, J.L. and Pichoir, F. (1985) PAP $\phi(\rho Z)$ procedure for improved quantitative microanalysis. In *Microbeam Analysis-1985*, 104–106. San Francisco Press, San Francisco, California.
- Udawaga, S., Urabe, K., and Hasu, H. (1974) The crystal structure of muscovite dehydroxylate. *Japanese Association of Mineralogists, Petrologists, and Economic Geologists*, 69, 381–389.

MANUSCRIPT RECEIVED MAY 5, 1999

MANUSCRIPT ACCEPTED NOVEMBER 1, 1999

PAPER HANDLED BY ANNE M. HOFMEISTER